

**INFLUENCE OF STRUCTURE AND SIZE OF CRYSTALLINE  
AGGREGATES ON THEIR COMPRESSION ABILITY**

**S. Veessler, R. Boistelle**

**CRMC2-CNRS**

**Campus de Luminy, case 913**

**13288 Marseille cedex 09, France**

**A. Delacourte, J.C. Guyot**

**Pharmacotechnie Industrielle**

**Faculté de Pharmacie, Lille, France**

**A.M. Guyot-Hermann**

**Pharmacie Galénique et Biopharmacie**

**Faculté de Pharmacie, Lille, France**

**ABSTRACT**

The compression abilities of polycrystalline aggregates exhibiting well defined mosaic or radial structures are studied, taking also into account strength and size distribution of the aggregates.

Six samples of alumina trihydrate, having different origins, crystallization history and mechanical strength, were selected, as this material grows under the form of nearly spherical aggregates and can be considered as a model substance.

The samples with radial structures are weaker materials with respect to the samples with mosaic structures as shown by attrition tests.

They have also a poorer compression ability, i.e. a smaller cohesion index, as shown by compression tests. On the other hand, inside the same type of structure, there is no direct correlation between cohesion index and attrition index.

The experiments also show that the smaller the aggregates are, the highest the cohesion index is, the improvement being more significant in the case of the mosaic structures.

By comparing the size distributions of the aggregates before and after compression it appears that the diameter of the particles is really affected only when the compression exceeds a critical value. These measurements, together with SEM observations, allow to understand the effect of compression on the different aggregate structures. In the case of a mosaic structure, compression induces the occurrence of one new population of particles, whereas in the case of a radial structure, compression induces the formation of two new populations of particles.

## 1. INTRODUCTION

There are many reports in literature dealing with the influence of particle size and size distribution on the compression ability. It is generally admitted that wide size distributions give rise to good compressions, the smallest particles being entrapped between the largest ones. In addition, when all the particles have nearly the same size in the sample, it is observed that compression of small particles usually results in the formation of stronger tablets than compression of large particles.

On the other hand, the influence of the exact nature of the particles (single crystals, aggregates) and of their structure is more open to discussion. Several aspects must be taken into consideration according to whether the chemical compound to be compressed may occur under different polymorphic modifications. If polymorphism exists, the compression ability of either form can be quite different, due to the internal arrangement of the molecules inside the unit cells of the crystals.

The forces applied onto the sample are not transmitted in the same way and gliding of the molecules is more or less difficult according to the crystal structure. On the other hand, when only one polymorphic modification exists or is available, compression is only affected, with respect to the previous case, by crystal habit, degree of crystallinity and agglomeration of the elementary particles. It has been shown for instance that the lower the degree of crystallinity is, the best the compressibility is [1]. It also seems that acicular and tabular habits cause bad flow properties and preferential orientation of the particles in the compression chamber.

The compression ability depends on the internal texture of the crystals. The texture can be defined as an arrangement of areas of matter, inside the elementary particle [2]. The more disordered the texture is, the best the compressibility is.

Some of us [3] have previously shown that a polycrystalline structure, exhibiting a sintered aspect had a very good compression ability. In the present study we aim at showing the different compression abilities of some polycrystalline structures with special attention to the influence of mosaic and radial structures. Influence of aggregate size, size distribution and aggregate solidity are taken into account.

## 2. MATERIALS

Gibbsite or hydrargillite, one of the different forms of crystallized alumina trihydrate ( $\text{Al}(\text{OH})_3$ ) was selected as a model substance for compression tests as it has some interesting characteristics.

In so far as industrial materials are concerned, gibbsite always crystallizes from caustic solutions under the form of nearly spherical aggregates. Actually, there are two steps in the crystallization process. In the first step, primary crystallites, the size of which is always less than 15  $\mu\text{m}$  collide and coalesce. In the second step, the small aggregates which have been formed grow and become coarser. However, according to the crystallization conditions, the arrangement of the particles inside the

aggregates may be quite different, giving rise to different aggregate structures. In the so-called American process, there is agglomeration of many particles and it is not necessary to grow them for a long period of time in order to produce aggregates of about 50  $\mu\text{m}$  in diameter or more. In the European process, there is agglomeration of a smaller number of particles so that a longer period of time is required to grow the aggregates up to a size of 50  $\mu\text{m}$ . As a result of these agglomeration and growth conditions, the former aggregates exhibit a mosaic structure whereas the latter ones exhibit a radial structure.

Figs. 1 and 2 show the external aspects of aggregates displaying mosaic and radial structures respectively. In addition, figs. 3 and 4 show the internal arrangement of the primary crystallites inside the mosaic and radial structures as they can be observed after immersion of the aggregates in aniline [4], a liquid which has nearly the same refractive index as the crystals.

Six different materials were used for the compression tests. They have all different origins, crystallization history and mechanical strength. Three of them, named A, B and C have mosaic structures whereas the three others, named D, E and F have radial structures.

In order to compare the influence of the structure and of the size of the aggregates, we carried out the compression tests on the raw materials and on three granulometric fractions obtained by wet sieving procedure :

below 63 $\mu\text{m}$	named f (as fine)
from 63 to 90 $\mu\text{m}$	named m (as medium)
from 90 to 125 $\mu\text{m}$	named c (as coarse)

So we obtain 24 different materials named for example A, Af, Am, Ac, ...

### 3. METHOD

**3.1 Attrition-** Another interesting characteristic of alumina trihydrate is that the aggregate structures induce different mechanical strengths. Actually, the solidity of the aggregates is also size dependent but to a

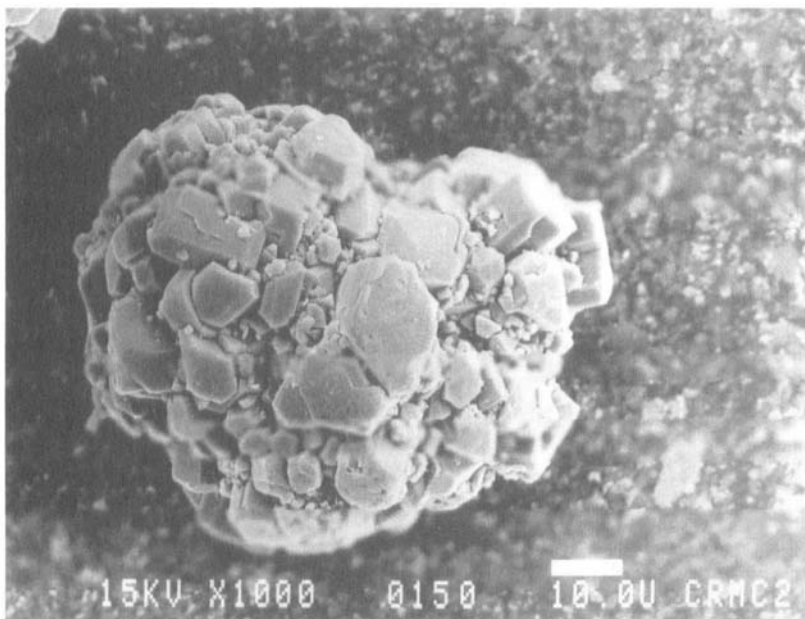


**FIGURE 1**

External aspect of aggregates displaying mosaic structure

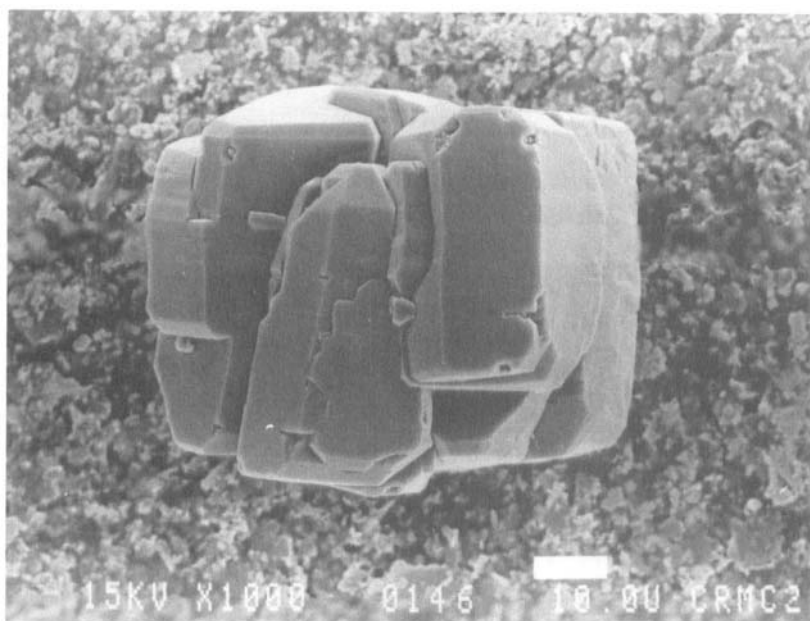


**FIGURE 2**

External aspect of aggregates displaying radial structure

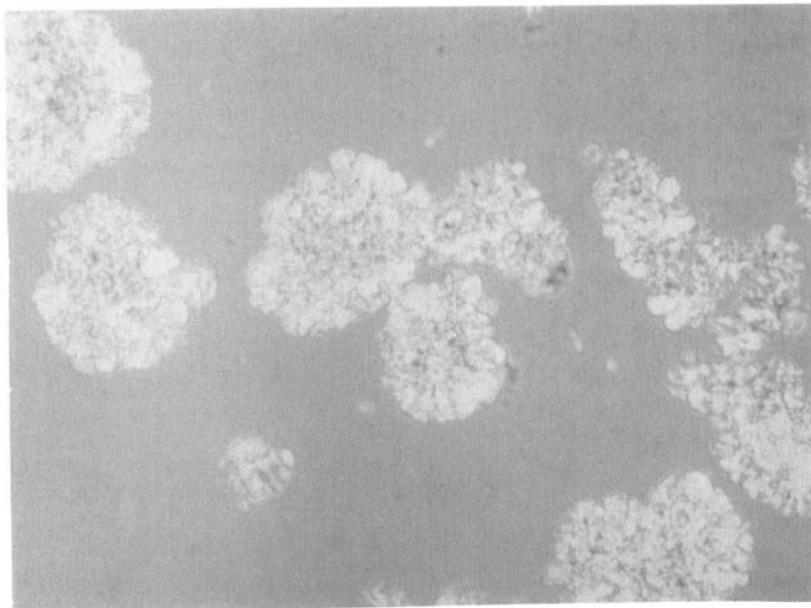


**FIGURE 3**

Internal arrangement of the primary crystallites inside the mosaic structure

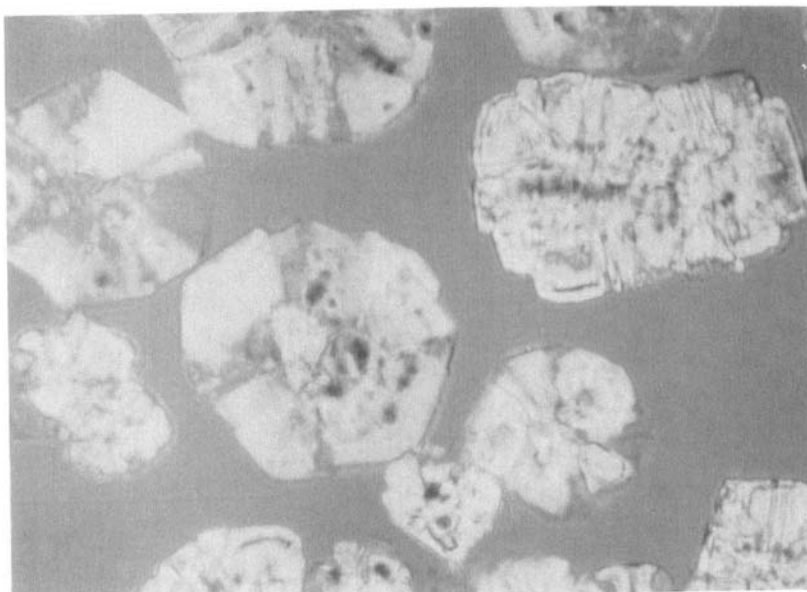


**FIGURE 4**

Internal arrangement of the primary crystallites inside the radial structure

small degree when similar size distributions of the aggregates are involved. Nowadays, solidity is quantified by means of an attrition test [5,6,7]. In this test, the material is poured into a vertical glass pipe and subjected to an air-jet which fluidizes the bed of solid particles. These ones are accelerated, collide and are more or less damaged according to the air velocity and to their mechanical strength. Attrition, or breakdown, occurs either by grinding or splitting of the aggregates.

The attrition index generally used [6] is the Alcoa Index (AI), being

$$AI = \frac{100(X-Y)}{100 - Y}$$

where X and Y are the percentages of solid particles smaller than 45  $\mu\text{m}$ , after (X) and before (Y) attrition. Accordingly, the smaller AI is the stronger the material is. In order to calculate the attrition index, it is necessary to determine the particle sizes before and after attrition. In our case, we used a Coulter Counter TA II or an Elzone PC 280 granulometer.

**3.2 Compression-** The ability to compression was estimated, for each sample, by a series of compression tests with an instrumental tablet machine.

The trials were made on a FROGERAIS OA single punch tablet machine using 1  $\text{cm}^2$  area flat punches. The upper and lower punches are instrumented with strain gauges calibrated against a reference device in a hydraulic press. A linear variable differential transformer measures the displacement of the upper punch inside the die with an accuracy of 1/100th of a mm. The strain gauges and the displacement transducer are connected to a computer by means of measuring bridges. This equipment gives, amongst other measurements, the possibility to know for each tablet the maximum forces Y1 and Y2 measured on the upper and lower punches and the maximum displacement X of the upper punch inside the die during compression [8].

For each compression test, the experimental conditions were the same :

- before weighting the powders, they are dried at 95°C for 1 hour and let to cool in the room where the compression tests are made. The relative humidity of this room is kept at 20% and its temperature at 20°C.
- the depth of the compression chamber is constant (1 cm  $\pm$  0.01)
- before each compression, the die and the punches are cleaned and lubricated by compression of ten tablets of a mixture of Avicel PH 102 and 0.5 % magnesium stearate placed in the hopper of the machine. Due to the low density of Avicel, the maximum displacement of the upper punch in the die must be adjusted between 6.5-7.5 mm range for obtaining sufficiently hard tablets.
- the weight of the sample of powder is constant : 650 mg  $\pm$  0.1 are weighted and poured by hand into the compression chamber. This amount has been chosen to obtain upper punch maximum forces between 1000 and 2000 daN with the maximum displacement range of the upper punch previously determined by the Avicel mixture used to clean and lubricate the die.
- for each batch, we compressed at least two samples at every ajustement of the eccentric and we carried out 3 to 5 different ajustements between 6.5 to 7.5 mm
- the machine is started by hand, but the speed of the punch in the die is controlled by the computer and kept constant for each experiment.

After each compression, the weight, the thickness and hardness of the tablet are measured by means of a Heberlein hardness tester. The compression ability is estimated by an adimensional number, the "Cohesion Index" (CI), ratio of the hardness (the force necessary for crushing the tablet) against the force measured during compression, multiplied by 10<sup>5</sup>. The higher the cohesion index is, the better the compressibility is [9].



#### 4. RESULTS AND DISCUSSION

In table 1 the attrition indices (AI) and median diameters ( $d_{50}$ ) are given for both the raw materials and the 63-90  $\mu\text{m}$  size range. It is noteworthy that E and F are rather weak materials (high AI), which is normal because radial structures are known to be weaker than mosaic structures. From this point of view, sample D is abnormally strong. Concerning the median sizes of the aggregates, we see that they are almost equal, once the samples have been sieved. As size distributions and median diameters are the same for the six samples, they have the same influence on the behaviour of the materials with respect to their compression ability.

Table 2 summarizes the CI calculated for a maximum displacement of 7.00 mm for all the samples.

We can observe that the results obtained with the mosaic structure are more regular than with the radial structure and that medium sized radial particles give a weaker cohesion index than coarse particles. The results, on the whole, are in correlation with the classical knowledge about the influence of the size of the particle on cohesion ; the finer the particles are, the higher the cohesion index is. But the improvement is more significant with mosaic structures.

The most important conclusion of this experiment is that the improvement in the cohesion observed is more a consequence of a modification in the structure of the particles than of a modification in their sizes.

Figure 5 shows the curve of CI as a function of the displacement of the upper punch in the case of the compression of the raw materials. It turns out that the compression ability of the mosaic structures is much better than that of the radial structures. This trend is still more pronounced in the case of the sieved materials. Figure 6 shows the corresponding representation for the 63-90  $\mu\text{m}$  size range.

Moreover, we do not observe any difference in the cohesion index in correlation with the attrition indices.

**TABLE 1. CHARACTERIZATION OF THE SIX SAMPLES OF ALUMINA TRIHYDRATE AGGREGATES BY THEIR ATTRITION INDEX AND MEDIAN DIAMETER**

Sample	Raw material : 10-120 $\mu\text{m}$		Size range : 63-90 $\mu\text{m}$	
	AI	$d_{50}$ ( $\mu\text{m}$ )	AI	$d_{50}$ ( $\mu\text{m}$ )
A	13	84.9	8	77.7
B	11	85.2	14	74.6
C	13	81.8	10	74.7
D	8	94.4	13	79.2
E	26	75.7	35	73.1
F	19	56.5	54	77.1

**TABLE 2. CI CALCULATED FOR A MAXIMUM DISPLACEMENT OF 7.00 MM**

Samples	Raw material	Fraction f	Fraction m	Fraction c
A	256	387	288	278
B	198	252	218	212
C	218	252	229	230
D	152	148	133	149
E	137	178	108	124
F	154	155	81	127

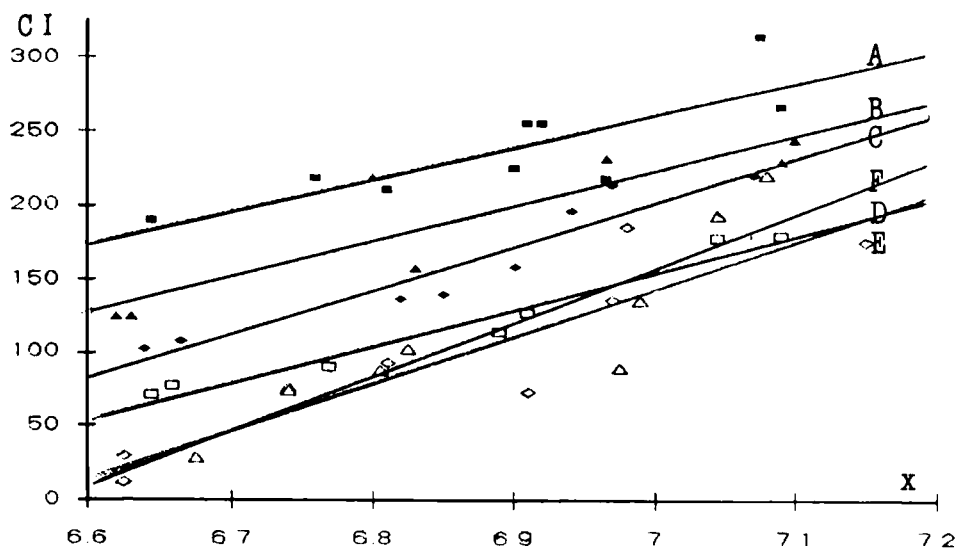


FIGURE 5

Cohesion index as a function of the displacement of the upper punch of the raw materials

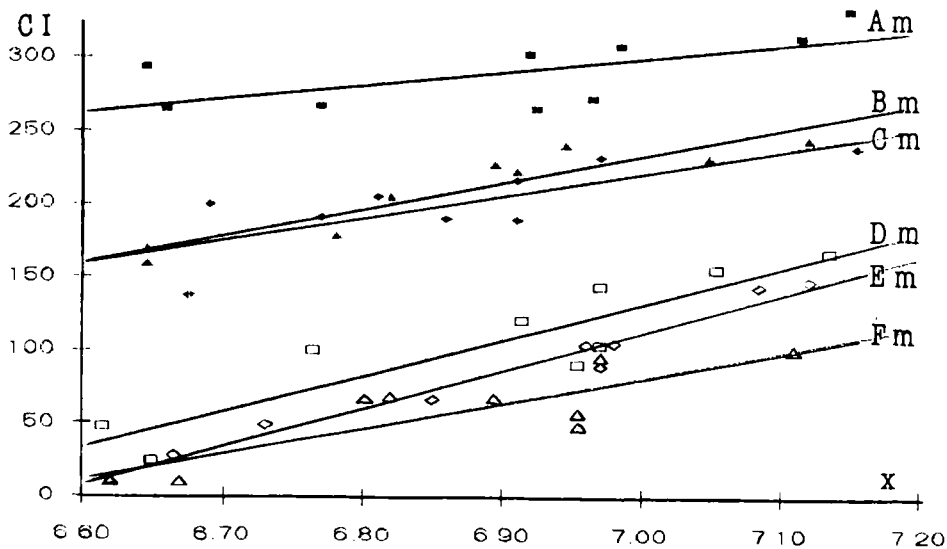


FIGURE 6

Cohesion index as a function of the displacement of the upper punch of fractions 63-90  $\mu$ m

**TABLE 3. CLOF MOSAIC SAMPLES WITH THE SAME SIZES  
AND DIFFERENT ATTRITION INDICES**

	Median size $\mu\text{m}$	Attrition index	Cohesion index for $x = 6.50$
MD 170	44.02	52	400
MD 191	44.29	60	380
MH 172	74.09	4	250
MH192	69.03	8	270

In order to have a new piece of information about this specific problem, we compress samples of mosaic structure with particles almost similar in size and different attrition index (table 3) in the same general condition as described above. It is noteworthy that the strength of the aggregates is significantly different even if the differences in the AI values seem to be small. This is confirmed by SEM observations. Obviously, those results confirm that the difference between the attrition indices has no influence on the cohesion index.

A possible explanation is the excessive level of forces developed during compression. The break of the particles may occur at the beginning of the compression for a very low level of forces. For better understanding of the behaviour of our crystalline materials, we determined the size distribution of the samples (initial size range : 63-90  $\mu\text{m}$ ) submitted to very low compression. For this experiment, we made different adjustments of the eccentric : at the beginning the powder was not compressed. Increasing the displacement, we obtained a tablet with zero hardness ; we have named this critical value "Point F"[10]. The lower the value of F is, the better the tableability is. Beyond this value, the hardness increases.

**TABLE 4. MAXIMUM UPPER PUNCH FORCE MEASURED (IN daN) FOR DIFFERENT UPPER PUNCH DISPLACEMENTS. THE VALUES MARKED WITH AN ASTERISK CORRESPOND TO THE CRITICAL VALUE F**

Upper punch maximum displacement (mm 10 <sup>-2</sup> )	525	550	600	625	650
A	113*	170	347	472	676
F			305*	417	562
D				343*	454

**TABLE 5. EVOLUTION OF THE MEDIAN DIAMETER  $d_{50}$  ( $\mu\text{m}$ ) OF THREE SAMPLES SUBJECTED TO COMPRESSION AS A FONCTION OF THE UPPER PUNCH MAXIMUM DISPLACEMENT. THE VALUES MARKED WITH AN ASTERISK CORRESPOND TO THE CRITICAL VALUE F**

Sample	Upper punch maximum displacement (mm 10 <sup>-2</sup> )						
	0	400	525	550	600	625	650
A	77.7	77.9	75.5*	75.9	75.1	75.4	71.8
F	77.1	-	-	76.5	74.7*	74.8	71.2
D	79.2	-	-	-	79.2	77.4*	76.7

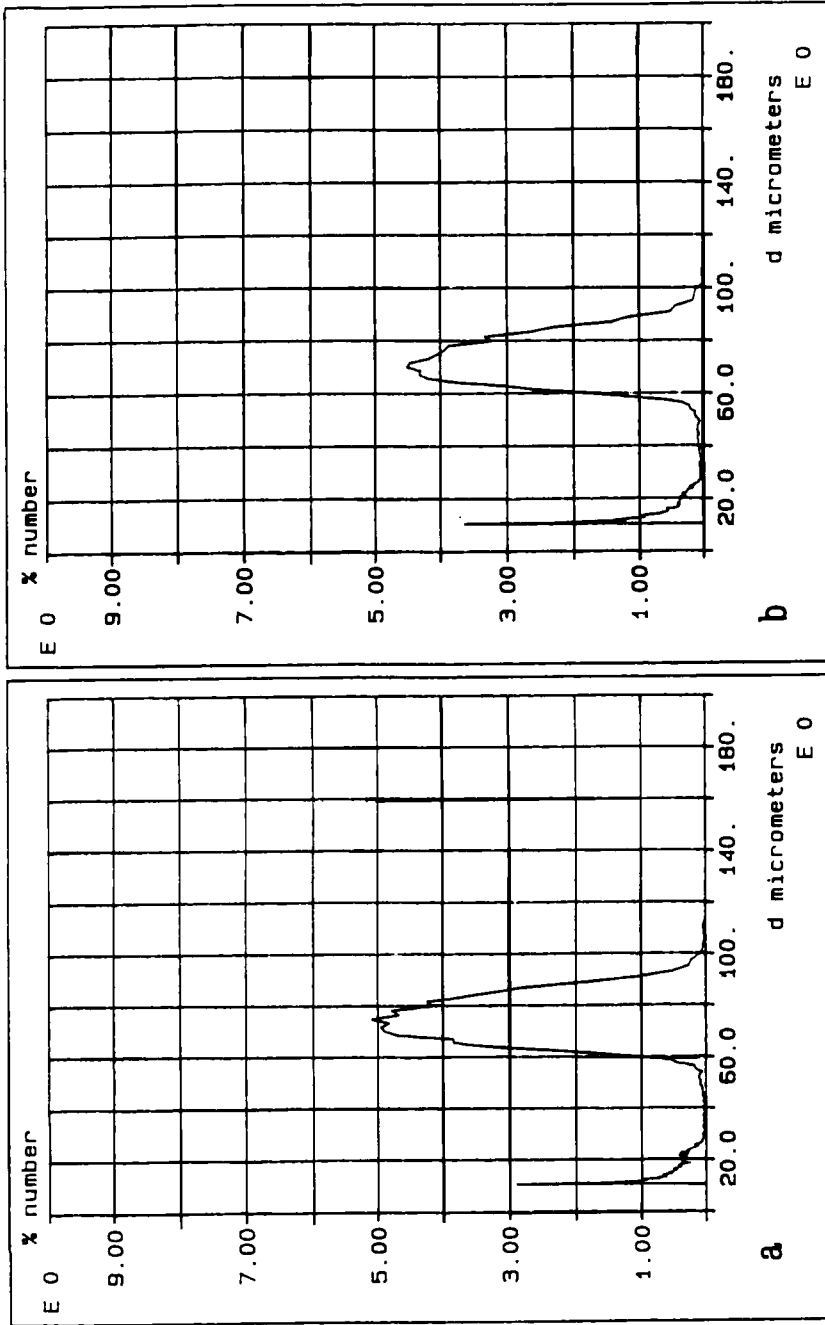


**FIGURE 7**

Size distribution curves (% number of particles versus size) before (a) and after (b) compression for the sample Am

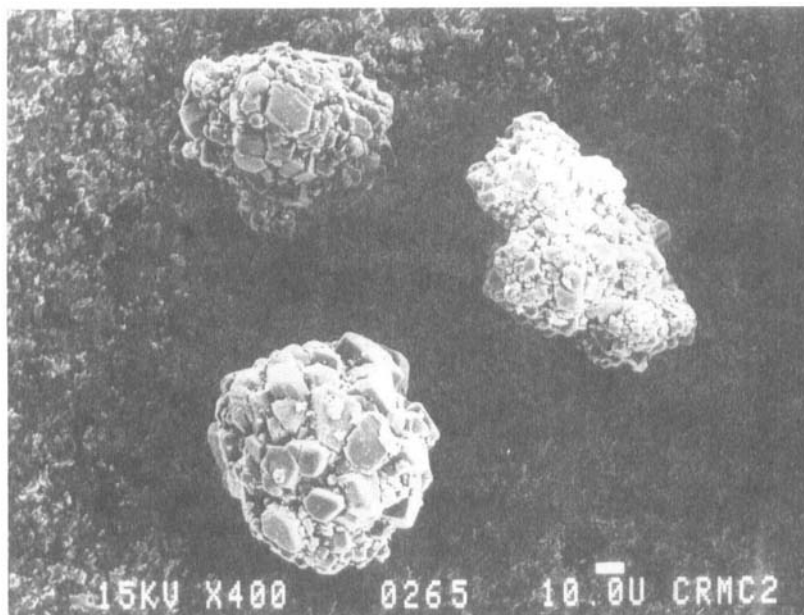


**FIGURE 8**

External shape of the aggregates sample Am

For this experiment, we chose two samples which exhibit mosaic (A) or radial (F) structures and have typical attrition indices (table 1). The case of sample D is also considered here due to its surprisingly small attrition index with respect to those of the two other radial structures E and F.

On the table 4, we can observe that the F value of the mosaic A (525) is lower than for the radial particles F (600) and D (625). This is in perfect correlation with the previous results on the better compression ability of the mosaic structure compared to the radial structure.

Table 5 gives the median diameters of the particles before and after that very low amplitude compression.

It appears that the median diameter of the particles is really affected only when the compression exceeds a critical value. For this critical

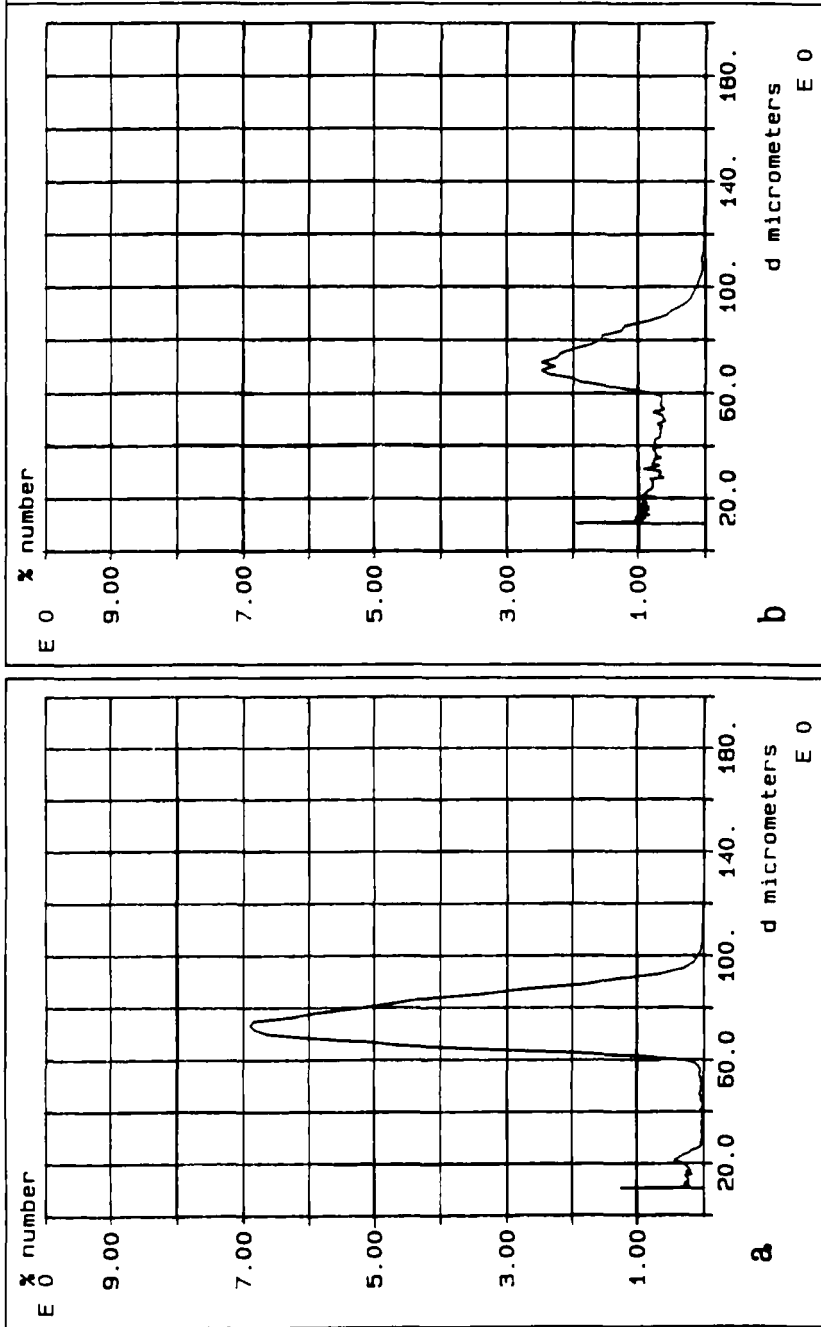


**FIGURE 9**

Size distribution curves (% number of particles versus size) before (a) and after (b) compression for the sample Fm



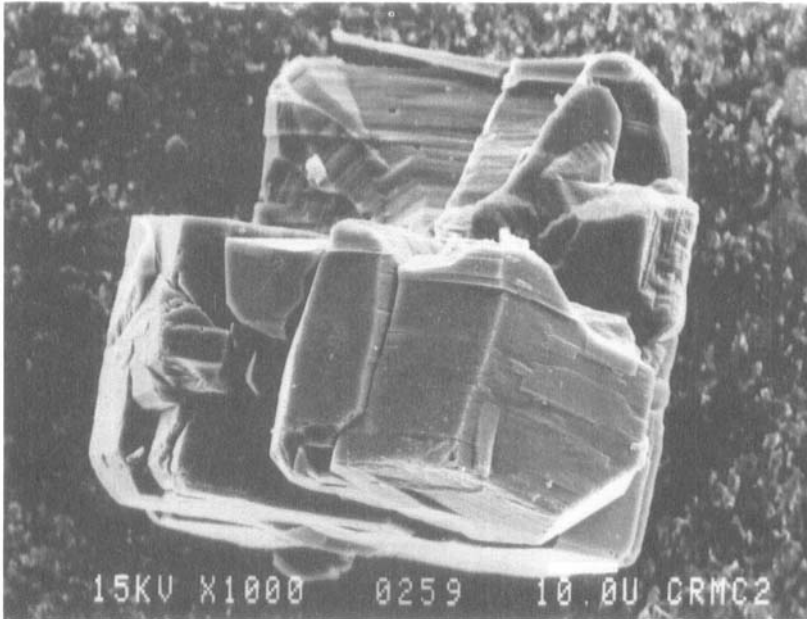


**FIGURE 10**

External shape of the aggregates sample Fm

value  $F$  we observe a break of the particles which is in correlation with the behaviour of the powders observed during compression.

To know more precisely what happens during compression we give in figures 7, 9 and 12 the complete size distribution curves (number of particles against size) before (a) and after (b) the samples have been subjected to a compression exceeding the critical value. All curves are normalized so that the sum of the % number is 100%. On the basis of the size and shape evolution of the particles, the following conclusions can be drawn.

- Strong mosaic structure A. Comparison of figures 7a and 7b shows that after compression, there are two distinct populations of particles. There are still many particles having the initial size (63 to 90  $\mu\text{m}$ ), beside new

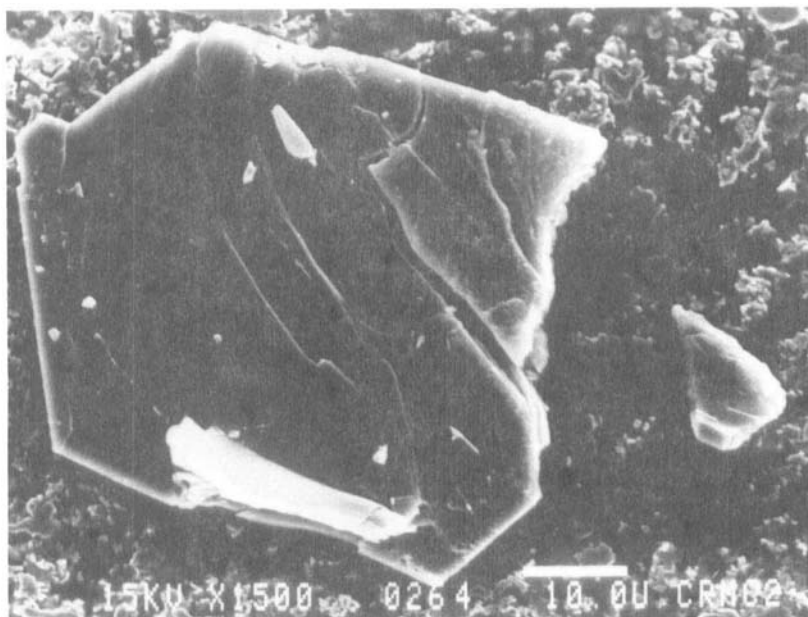


**FIGURE 11**

External shape of the aggregates sample Fm

crystallites the size of which ranges from 10 to 15  $\mu\text{m}$ , which is the size of the primary crystallites agglomerated during the first step of the crystallization process. The external shape of the aggregates and their sizes is not really affected by compression as shown in figure 8. Only a few crystallites have been pulled out from the aggregates and none was further split into smaller parts. It may be seen that the maximum value of the peak (at 70  $\mu\text{m}$ ) changes from 5% (fig. 7a) to 4.5 % (fig. 7b). The secondary maximum (10  $\mu\text{m}$ ) increases from 1% (fig. 7a) to 2% (fig. 7b).

- Weak radial structure F. The behaviour of this material is quite different as it may be seen by comparing figures 9a and 9b. Compression induces two new populations of particles beside the population of 63 to 90  $\mu\text{m}$ . The first one consists of particles ranging from 20 to 63  $\mu\text{m}$  which were pulled out from the aggregates. This can be seen in figure 10 which

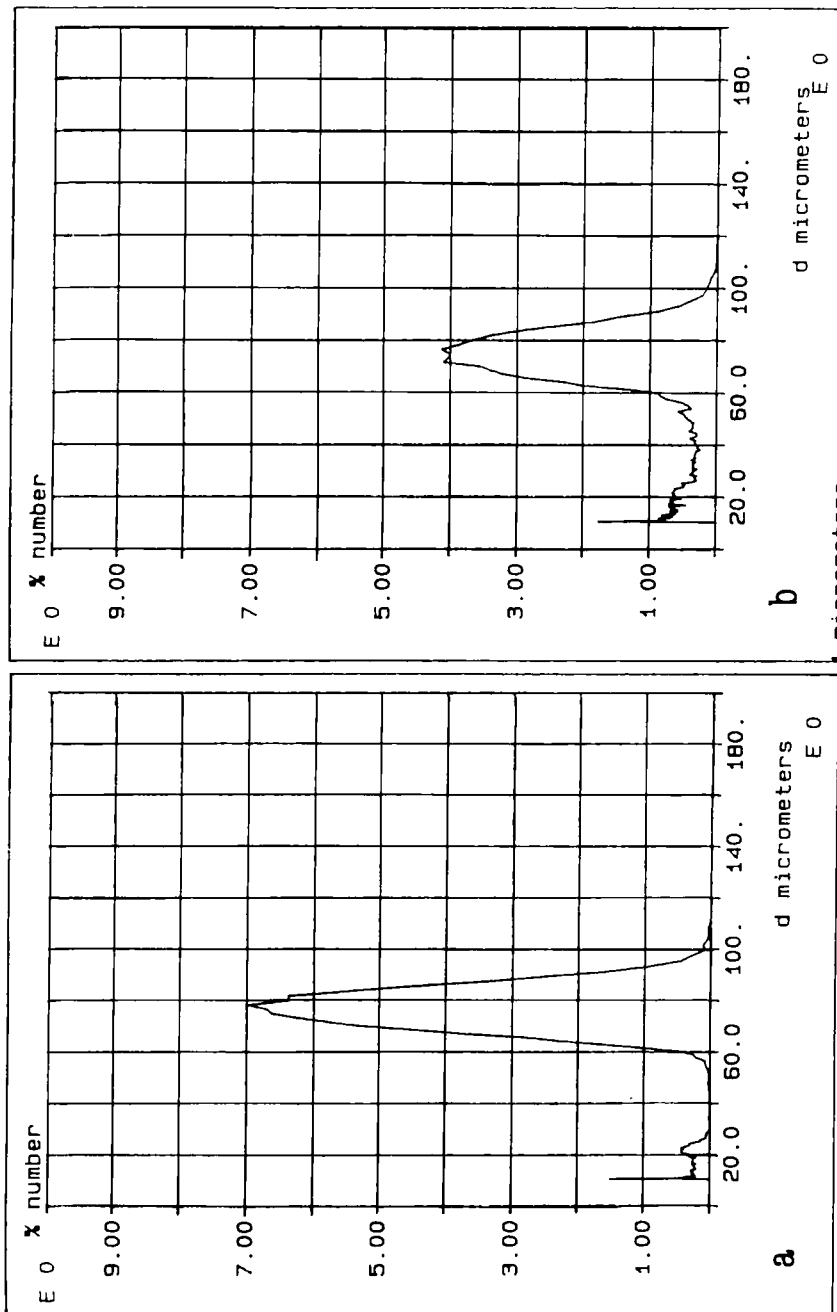
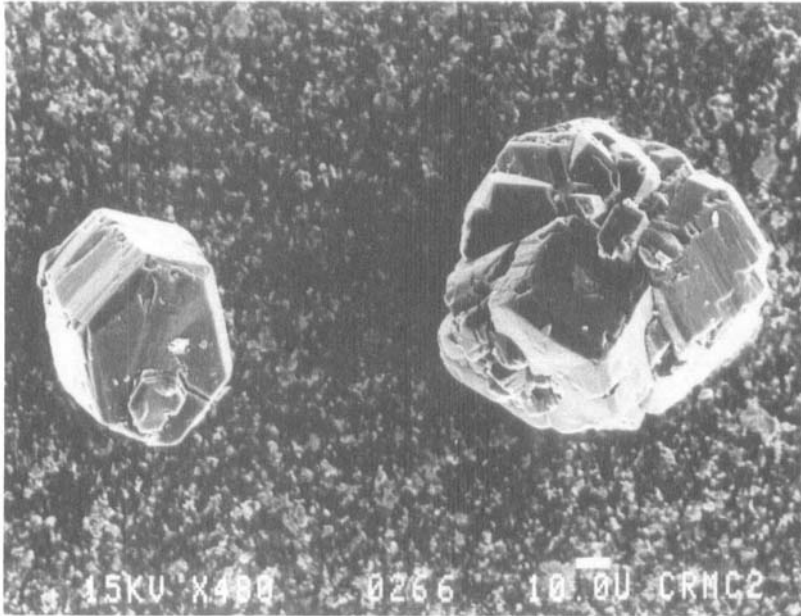


FIGURE 12

Size distribution curves (% number of particles versus size) before (a) and after (b) compression for the sample Dm



**FIGURE 13**

External shape of the aggregates sample Dm

A  
B  
C  
D  
E  
F

Am  
Bm  
Cm  
Dm  
Em  
Fm

shows that an important block has been removed from the upper part of the aggregate. Growth layers, starting from the core of the remaining primary crystal, can be observed in this area. In the lower part of figure 10 we also note the existence of cleavage planes generated by the force applied onto the sample. Once the primary crystallites have been separated from the aggregate, they can subsequently split into smaller particles (fig. 11). This gives rise to the second new population of particles, the size of which ranges from 10 to 20  $\mu\text{m}$ .

- Abnormal strong radial structure D. If we compare figure 12b and 12a, we find once more the initial particles of 63 to 90  $\mu\text{m}$ . This means that the behaviour of sample D is closer to that of A than to that of F despite the fact that F has the same structure as D. Primary crystallites are removed from the initial aggregates but they do not split into smaller particles (fig. 13).

## 5. CONCLUSION

Thanks to this model, we have demonstrated the importance of the structure of crystalline aggregates on their compression ability. The mosaic particles, which have a more disordered texture than the radial particles, have a much better compression ability. The cohesion index, which is very sensitive, is convenient to choose the best structure in correlation with compression and is affected by the size of the polycrystalline particles. We have demonstrated that those polycrystalline particles break under very low stresses.

## ACKNOWLEDGEMENTS

The authors are indebted to Mrs M.C. Toselli for technical assistance and to ALUMINIUM PECHINEY for financial support.

## REFERENCES

1. R. Hüttenrauch, Pharm. Ind., 45, 4, 435-440 (1983)

2. M. Figlarz, F. Vincent, L. Lecaille, J. Amiel, *Powder Technol.* 1 121-128 (1967)
3. C. Lefèbvre, A.M. Guyot-Herman, J.C. Guyot, R. Bouché, J. Ringard, *8th Pharm. Technol. Conf. Monte-Carlo* (1989)
4. G.I.D. Roach, J.B. Cornell & A. Antonovsky, *Smelter Grade Alumina for the 1990's and Beyond*, Gladstone, Queensland, Australia, September 1988
5. W.L. Forsythe, Jr., & W.R. Hertwig, *Indust. Engineer. Chem.* 41 (6) 1200-1206 (1949)
6. J.L. Anjier & D.F.G. Marten, *Light Metals*, 199-209 (1982)
7. M. Remillard, L. Cloutier & J.C. Methot, *Can. J. of Chem. Engineer.* 56 230-235 (1978)
8. J.C. Guyot, A. Delacourte & B. Marie, *Drug Dev. Ind. Pharm.* 12 1869-1884 (1986)
9. J.C. Guyot, A. Delacourte, P. Leterme & P. Billardon, *STP Pharma* 5 168-175 (1989)
10. J.C. Guyot, A. Delacourte, B. Devise & M. Traisnel, *Labo Pharma* 263 209-214 (1977)